Volume 22, No 3 | International Journal of Radiation Research, July 2024

Spread-out of Bragg peak of proton beam using Au nanoparticles: A Monte Carlo simulation study

A.S. Talebi* **and H. Rajabi**

Department of Medical Physics, Faculty of Medical Sciences, Tarbiat Modares University, Tehran, Iran

► ***Original article***

Corresponding author:
Asra Sadat Talebi,
E-mail:
asra.talebi@modares.ac.ir

Received: November 2023
Final revised: February 2024
Accepted: February 2024

Int. J. Radiat. Res., July 2024; 22(3): 697-701

DOI: 10.61186/ijrr.22.3.697

Keywords: *Bragg peak, Proton, Au nanoparticle, Monte Carlo, SOBP.*

ABSTRACT

Background: Proton Beam Therapy (PBT) provides significantly enhanced dose distribution and dosimetric advantages compared to photon beam radiation therapy. In PBT, the Spread-Out Bragg Peak (SOBP) is crucial for achieving a conformal dose distribution within the target volume. We propose a novel method for creating SOBP by passing the beam through slabs containing varying concentrations of Au nanoparticles (NPs). ***Materials and Methods:*** GEANT4.10.6 was used for Monte Carlo tracking of proton beams within the slabs and water phantom. Various arrangements of layers containing AuNPs, with concentrations ranging from 1 to 35 M, were positioned along the path of the proton beams with an energy of 200 MeV. The most suitable arrangement of the slabs was determined based on the width of the SOBP and the dose variation in the SOBP plateau. ***Results:*** In the most suitable quintuple and sextuple arrangements of slabs, the width of the Bragg peak increases within the range of 45 to 65 mm. Furthermore, in these arrangements, variations in dose within the SOBP plateau are less than 5%. ***Conclusion:*** The arrangement of slabs with different AuNP concentrations is a stationary device placed along the beamline. This setup requires no additional time considerations and can be readily incorporated within the clinical setting.

INTRODUCTION

The proton beam offers advantages over the photon beam in treating various cancers, such as esophageal squamous cell carcinoma, non-small cell lung cancer, and deep-seated chordomas [1-4]. This is primarily due to the more precise dose localization and higher biological effectiveness of the cells near the Bragg peak, which enhances the therapeutic efficiency of Proton Beam Therapy (PBT) [5,6]. The potential benefit of PBT is associated with the energy distribution of the traversed matter, which differs significantly from that of photon beams [7,8]. The energy loss of the proton beam increases to a peak value and then decreases rapidly. Because of this unique physical characteristic, there is a region of maximum dose along the beam's path of the protons called the Bragg peak [9,10]. The depth of the Bragg peak depends on the initial kinetic energy of the protons.

When the Bragg peak is over the region of interest, the maximum dose is delivered to the target cells, while normal cells receive lower energy. A proton beam deposits its energy almost entirely at the end of the particle's path in the matter, resulting in a sharp decline in the dose. This energy distribution benefits conformal radiation therapy and can reduce treatment-related toxicities [11].

A monoenergetic proton beam is unsuitable for treating large cancer tumors due to the narrow width of the Bragg peak. The Bragg peak's width in the depth dose profile ranges from 3 to 20 mm in the energy range of 60 to 200 MeV, which is insufficient for covering larger target volumes [12]. Spreading the Bragg peak helps extend the application of proton beams and provides better conformal doses for large tumors.

Both passive scattering and active scanning techniques are commonly used for Spread-Out Bragg Peak (SOBP) formation [13]. The passive scattering technique spreads the beam by introducing a set of range modulator wheels or ridge filters into the beam's path [14]. The active scanning technique uses fast-steering magnets to vary the proton beam's initial kinetic energy [15,16]. However, these SOPB techniques have their limitations. Significant effort is required to define the modulating devices in the passive scattering technique to achieve a 3D-conformal dose distribution. In the active scanning technique, switching the initial energy of the beams increases the irradiation time [17].

In recent years, nanoparticles (NPs) have been investigated for clinical applications ranging from diagnostics to disease control [18,19]. Among NPs, AuNPs have been extensively studied due to their unique biological properties [20,21]. NPs can effectively spread the Bragg peak by passing the proton beam through a solution containing NPs. This approach offers advantages such as ease of implementation and avoidance of increased irradiation time. However,

[DOI: 10.61186/ijrr.22.3.697]

until now, no investigation has examined the SOBP caused by AuNPs. In this study, we explore the SOBP phenomenon when utilizing layers containing gold NPs at various concentrations, employing a powerful simulation toolkit capable of simulating physical processes up to several electron volts.

MATERIALS AND METHODS

GEANT4.10.6 was used for Monte Carlo (MC) simulations of proton transport in a medium containing AuNPs [22]. GEANT4 is open-source code that is freely available for tracking nanoscale particles inside materials. The binary cascade (QGSP_BIC_EMY) model in Livermore physics was used to consider nuclear interactions of protons with AuNPs [23].

In the GEANT4 code, a water slab with dimensions of x = 0.4 cm, y = 2 cm, and z = 2 cm was taken into account. Various concentrations of AuNPs were integrated into these slabs. This study employed a series of 35 water slabs, each containing different concentrations of AuNPs ranging from 1M to 35M. AuNPs were considered to be a mixture of Au atoms inside the water slab. A proton beam with an energy of 200 MeV was uniformly directed at the water slab, which had dimensions of x = 0.4 cm and y = 2 cm. Bragg curves were calculated in the water phantom (x = 4 cm, y = 4 cm, z = 40 cm) for each slab with different concentrations of AuNPs. A total of 107 protons were considered to have acceptable uncertainty (< 2%). The energy cutoff range and step size were 0.1 mm for all particles.

The Bragg curves from the slabs containing various concentrations of AuNPs were combined using MATLAB version R2020b. In various combinations derived from layers with different AuNP concentrations, 2 fundamental criteria were assessed to select the most suitable arrangement. These criteria encompassed the SOBP width and the dose variation. Ideally, the optimal arrangement would demonstrate the maximum SOBP width and minimal dose variation in the SOBP plateau. The SOBP width refers to the width of the flat dose area above 90% of the maximum dose.

Figure 1 schematically illustrates the proposed method. Four water slabs with varying concentrations of 1M, 5M, 10M, and 15M are individually exposed to proton beams with an energy of 200 MeV to validate this method. The obtained Bragg peak curves from each water slab are summed together. In the subsequent stage, these 4 layers are placed side by side. This configuration is simultaneously exposed to a proton beam with an energy of 200 MeV, and the Bragg peak curve is calculated. For validation, the cumulative Bragg peak curves of the 4 layers will be compared to the Bragg peak curve resulting from the 4-layer configuration.

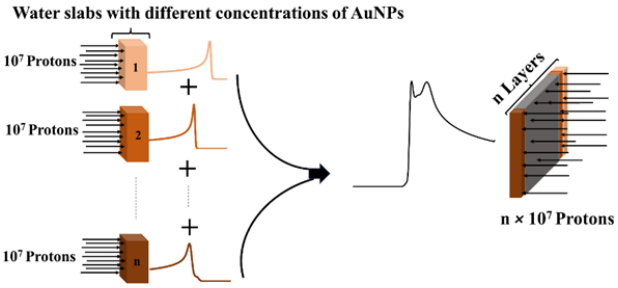

Figure 1. A sketch of the SOPB with the water slabs with different concentrations of AuNPs.

The difference between the cumulative Bragg peak curves of the 4 individual layers with the Bragg peak curve that emerges from the configuration of all 4 layers combined is shown in figure 2. The Bragg peak curves obtained in both scenarios are in excellent agreement.

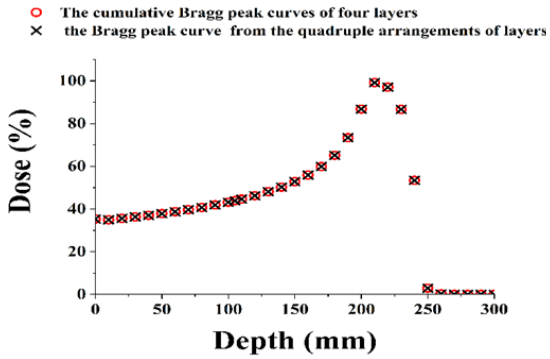

Figure 2. The difference between the cumulative Bragg peak curves of four individual layers with the Bragg peak curve that emerges from the combined configuration of all four layers.

Figure 3 shows the Bragg peak curves when layers with different concentrations of AuNPs were introduced along the path of the proton beam. As the concentration of AuNPs increases, the attenuation of the proton beam by the NPs leads to a reduction in the depth of the Bragg peak.

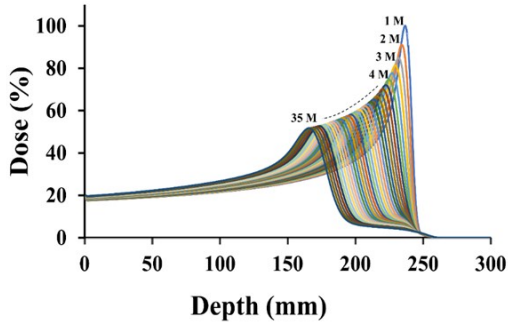

Figure 3. The Bragg peak curves for different concentrations of AuNPs.

Figure 4 shows the triple arrangements of slabs placed in the path of 200 MeV proton beams. The maximum width of the Bragg peak in the triple arrangements is 83 mm. In all the triple arrangements, the dose variation in the SOBP plateau region is approximately 30%. The Bragg peak associated with quadruple arrangements of slabs is

[DOI: 10.61186/ijrr.22.3.697]

illustrated in figure 5. The maximum width of the Bragg peak in quadruple arrangements is 76 mm. Additionally, the dose variation in the SOBP plateau region for the quadruple arrangements is less than 20%.

Figure 6 shows the most appropriate quintuple arrangements of slabs placed in the path of 200-MeV proton beams. In the presence of proper quintuple configurations of slab arrangements, incorporating various concentrations of AuNPs, the width of the Bragg peak increases within the range of 45 to 66 mm. Furthermore, in these arrangements, variations in dose within the SOBP plateau are less than 5%.

Figure 7 shows the most appropriate sextuple arrangements of slabs. The maximum and minimum widths of the Bragg peak in the sextuple arrangements are 65 and 48 mm, respectively. In all sextuple arrangements of slabs depicted in figure 7, the dose variation in the SOBP plateau region is less than 5%.

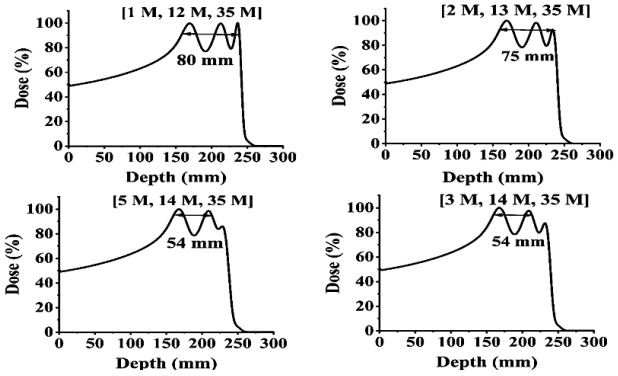

Figure 4. The Bragg for triple arrangements of layers containing AuNPs with different concentrations.

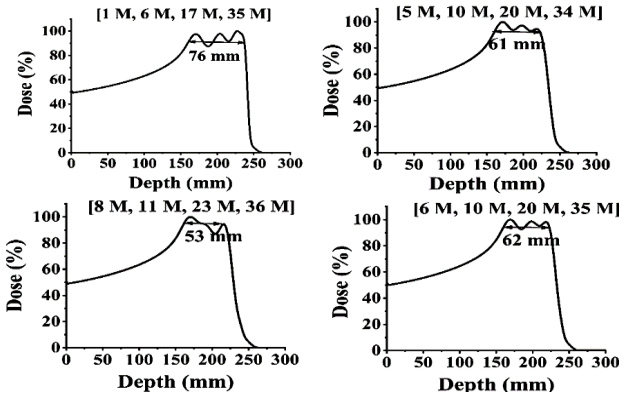

Figure 5. The Bragg for quadruple arrangements of layers containing AuNPs with different concentrations.

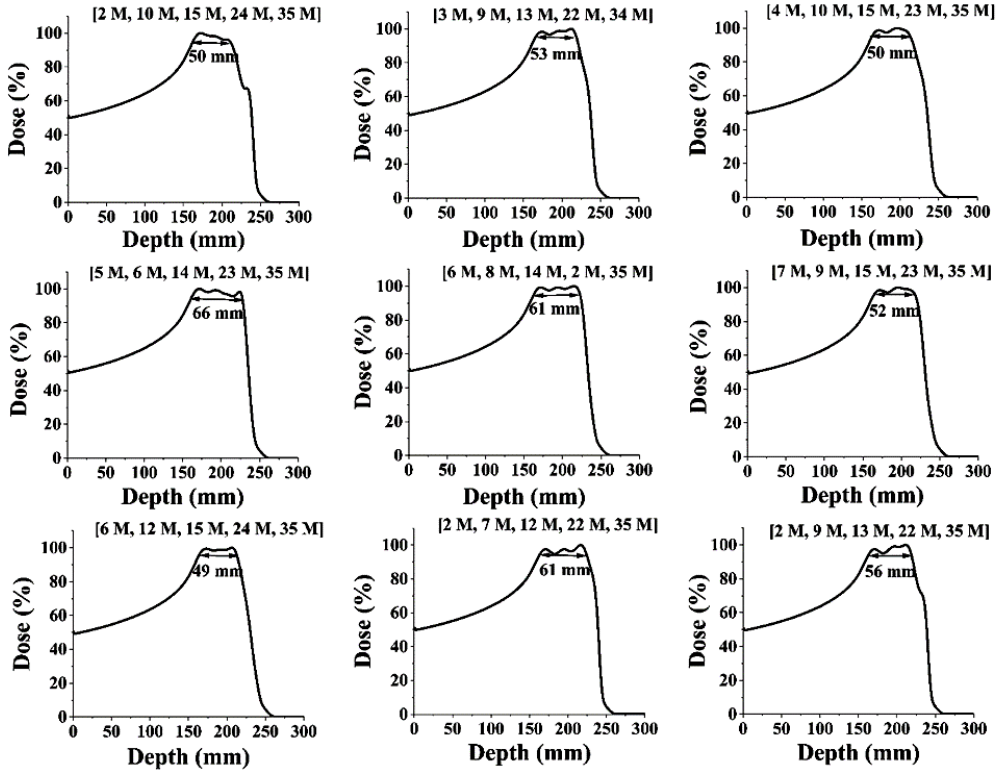

Figure 6. The Bragg for quintuple arrangements of layers containing AuNPs with different concentrations.

[DOI: 10.61186/ijrr.22.3.697]

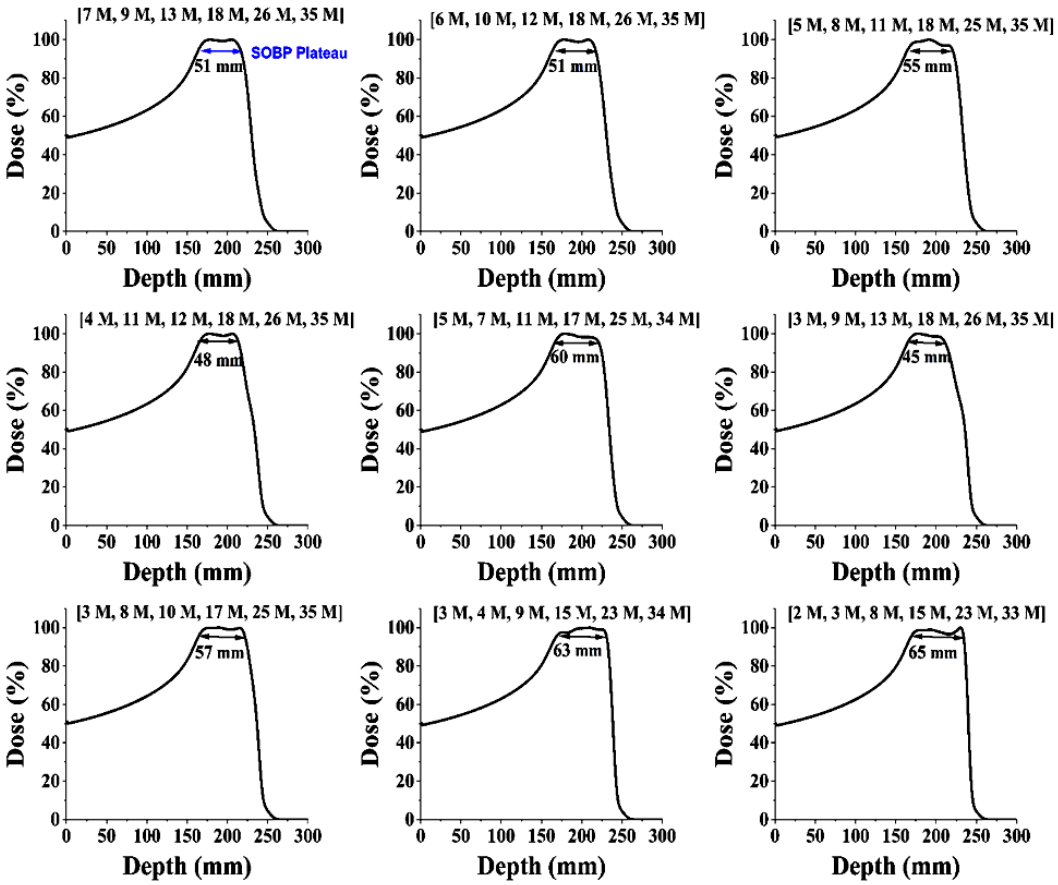

Figure 7. The Bragg curve for sextuple arrangements of layers containing AuNPs with different concentrations.

DISCUSSION

Robert Wilson suggested PBT in 1946, with the first patient being treated in 1954 [24,25]. In harnessing the benefits of PBT, achieving a conformal dose field stands as a pivotal objective. The distinctive feature of a proton particle beam lies in the characteristic distribution of the mono-energetic beam, commonly known as the Bragg peak. While this offers a precisely defined dose field, it necessitates meticulous energy control to attain the desired dose distribution. This intricacy sets particle therapy apart from conventional X-ray therapy, underscoring the need for sophisticated systems and highlighting the nuanced challenges associated with precision in energy management. As mentioned above, a monoenergetic proton beam is unsuitable for treating large tumors due to the narrow width of the Bragg peak. Broadened Bragg peaks are better suited for use in PBT. Passive scattering and active scanning techniques are employed for broadened Bragg peaks and energy management [13,26]. Previously conducted studies mainly focused on the design of ripple filters, ridge filters, and algorithms for modulating the intensity of proton beams [12,27,29]. The proposed SOBP techniques are complex, expensive, and extend overall irradiation times [26].

In our current investigation, we employed a straightforward approach to create SOBP. We propose the utilization of slabs containing varying concentrations of AuNPs, resulting in reduced irradiation duration and enhanced treatment efficiency. This method is sufficiently uncomplicated, enabling its implementation at any facility due to its minimal computational requirements. Embedding the slab of AuNPs with varying concentrations in the proton beam path leads to the generation of the Bragg peak at different depths. The superimposition of the various Bragg peaks leads to SOBP [26]. The flatness of the dose in the Bragg peak should also be considered when choosing the best arrangements of the slabs. For example, using a triple and quadruple arrangement of the slabs broadens the Bragg peak; however, the dose variation in the SOBP plateau exceeds 5%. These arrangements are unsuitable for PBT due to the lack of dose homogeneity in the Bragg peak.

Increasing the number of slabs leads to better smoothing of SOBP. Figures 4 - 7 show that the dose variations within the SOBP plateau are less pronounced in the quintuple and sextuple arrangements compared to the triple and quadruple arrangements. Moreover, increasing the number of slabs does not necessarily lead to an increase in the width of Bragg peaks. As mentioned above, the most suitable configuration exhibits a maximum Bragg peak width and a minimum dose variation in the SOBP plateau. Hence, despite their broad Bragg peaks due to significant dose variations, the triple and quadruple configurations are deemed unsuitable for

[DOI: 10.61186/ijrr.22.3.697]

the SOBP due to the substantial dose fluctuations in the SOBP plateau.

The discussion emphasizes the trade-offs between Bragg peak width and dose homogeneity in the SOBP plateau, culminating in the identification of quintuple and sextuple arrangements as optimal configurations. These configurations offer expanded Bragg peaks while maintaining dose uniformity, providing valuable insights for optimizing PBT efficacy. The study's findings contribute to the ongoing exploration of innovative approaches in the design of proton therapy configurations.

CONCLUSION

Our findings demonstrate a significant advancement in modulating Bragg peak characteristics by employing a specific arrangement of slabs, each with a uniform thickness of 4 mm, strategically placed along the path of proton beams. The observed outcome reveals a noteworthy expansion in the width of the Bragg peak, spanning from 45 to 80 mm. This broadening effect is contingent upon the concentration of NPs within the slabs. Furthermore, the applicability of this technique extends beyond proton therapy, as it can also be seamlessly incorporated into hadron therapy involving heavy ion beams. This versatility underscores the broader impact of our methodology, paving the way for enhanced control and customization in therapeutic interventions across different modalities.

Statement of conflict of interest: The authors declare that there is no conflict of interest regarding the publication of this article.

Funding: This work didn't receive any financial support.

Ethical consideration: This article does not contain any studies with human participants or animals performed by any of the authors.

Authors' contribution: H.R. designed the study. A.S.T. collected the data and wrote draft of the manuscript.

REFERENCES

1. Gordon K, Gulidov I, Koryakin S, Smyk D, Makeenkova T, Gogolin D, *et al*. (2021) Proton therapy with a fixed beamline for skull-base chordomas and chondrosarcomas: outcomes and toxicity. *Radiation Oncology,* ***16(1):*** *238.*
2. Gergelis KR, Jethwa KR, Tryggestad EJ, Ashman JB, Haddock MG, Hallemeier CL (2020) Proton beam radiotherapy for esophagus cancer: state of the art. *J Thorac Dis,* ***12(11):*** *7002-10.*
3. Brooks ED, Ning MS, Verma V, Zhu XR, Chang JY (2019) Proton therapy for non-small cell lung cancer: the road ahead. *Transl Lung Cancer Res,* ***8(Suppl 2):*** *S202-S212.*
4. Kim JK, Leeman JE, Riaz N, McBride S, Tsai CJ, Lee NY (2018) Proton Therapy for Head and Neck Cancer. *Curr Treat Options Oncol,* ***19 (6):*** *28.*
5. Mohan R, Peeler CR, Guan F, Bronk L, Cao W, Grosshans DR (2017) Radiobiological issues in proton therapy. *Acta Oncol,* ***56(11):*** *1367 -1373.*
6. Willers H, Allen A, Grosshans D, McMahon SJ, von Neubeck C, Wiese C, *et al.* (2018) Toward A variable RBE for proton beam therapy. *Radiother Oncol,* ***128(1):*** *68-75.*
7. Yuan T-Z, Zhan Z-J, Qian C-N (2019) New frontiers in proton therapy: applications in cancers. *Cancer Communications,* ***39(1):*** *61.*
8. Hu M, Jiang L, Cui X, Zhang J, Yu J (2018) Proton beam therapy for cancer in the era of precision medicine. *Journal of Hematology & Oncology,* ***11(1):*** *136.*
9. Jones D (1998) Present status and future trends of heavy particle radiotherapy. *Cyclotrons and their Applications, 13-20.*
10. Mohan R, Grosshans D (2017) Proton therapy - Present and future. *Adv Drug Deliv Rev,* ***109:*** *26-44.*
11. Romesser PB, Cahlon O, Scher E, Zhou Y, Berry SL, Rybkin A, *et al*. (2016) Proton beam radiation therapy results in significantly reduced toxicity compared with intensity-modulated radiation therapy for head and neck tumors that require ipsilateral radiation. *Radiother Oncol,* ***118(2):*** *286-292.*
12. Jia SB, Romano F, Cirrone GAP, Cuttone G, Hadizadeh MH, Mowlavi AA, *et al*. (2016) Designing a range modulator wheel to spread-out the Bragg peak for a passive proton therapy facility. Nuclear Instruments and Methods in Physics Research Section A: *Accelerators, Spectrometers, Detectors and Associated Equipment,* ***806:*** *101-108.*
13. Newhauser W (2009) International commission on radiation units and measurements report 78: Prescribing, recording and reporting proton-beam therapy. *Oxford University Press.*
14. Chu W, Ludewigt B, Renner T (1993) Instrumentation for treatment of cancer using proton and light-ion beams. *Review of Scientific Instruments,* ***64(8):*** *2055-2122.*
15. Kraft G (2000) Tumor therapy with heavy charged particles. *Progress in Particle and Nuclear Physics,* ***45:*** *S473-S544.*
16. Kanai T, Kawachi K, Kumamoto Y, Ogawa H, Yamada T, Matsuzawa H, *et al*. (1980) Spot scanning system for proton radiotherapy. *Med Phys,* ***7(4):*** *365-369.*
17. Bourhaleb F, Attili A, Russo G (2011) Monte carlo simulations for beam delivery line design in radiation therapy with heavy ion beams. *Applications of Monte Carlo Methods in Biology, Medicine and Other Fields of Science.*
18. Abbasi Kajani A, Haghjooy Javanmard S, Asadnia M, Razmjou A (2021) Recent Advances in Nanomaterials Development for Nanomedicine and Cancer. *ACS Appl Bio Mater,* ***4(8):*** *5908-5925.*
19. Abdel-Mageed HM, AbuelEzz NZ, Radwan RA, Mohamed SA (2021) Nanoparticles in nanomedicine: a comprehensive updated review on current status, challenges and emerging opportunities. *J Microencapsul,* ***38(6):*** *414-436.*
20. Medici S, Peana M, Coradduzza D, Zoroddu MA (2021) Gold nanoparticles and cancer: Detection, diagnosis and therapy. *Semin Cancer Biol,* ***76:*** *27-37.*
21. Talebi AS, Rajabi H, Watabe H (2022) Role of nanoparticles in transarterial radioembolization with glass microspheres. *Annals of Nuclear Medicine,* ***36(5):*** *479-487.*
22. Agostinelli S, Allison J, Amako Ka, Apostolakis J, Araujo H, Arce P, *et al*. (2003) GEANT4-a simulation toolkit. Nuclear instruments and methods in physics research section *A: Accelerators, Spectrometers, Detectors and Associated Equipment,* ***506(3):*** *250-303.*
23. Hamad MK (2021) Bragg-curve simulation of carbon-ion beams for particle-therapy applications: A study with the GEANT4 toolkit. *Nuclear Engineering and Technology,* ***53(8):*** *2767-2773.*
24. Wilson RR (1946) Radiological Use of Fast Protons. *Radiology,* ***47 (5):*** *487-491.*
25. Lawrence JH (1957) Proton irradiation of the pituitary. *Cancer,* ***10 (4):*** *795-798.*
26. Shao W, Tang X, Geng C, Shu D, Gong C, Zhang X, *et al*. (2020) Investigation of irregular radiation field-based proton therapy using conformal dose layer stacking method. *International Journal of Radiation Research,* ***18(2):*** *295-306.*

[DOI: 10.61186/ijrr.22.3.697]